

# The Fracture Distribution in ITO Coating with Compressive Bending Stress on Polymer Substrates

Sang-Keuk Lee\* and Joon-Ung Lee

*Department of Electrical Engineering, College of Engineering,  
Kwangwoon University, Wolgye-dong, Nowon-ku, Seoul 447-1, Korea*

\*E-mail : [aramis71@hanmail.net](mailto:aramis71@hanmail.net)

(Received 23 September 2003, Accepted 1 November 2003)

In this paper, we investigated the fracture distribution in indium-tin-oxide (ITO) coating with compressive bending stress on polymer. Under compressive strain, the ITO island delaminates, buckles and cracks. As the mechanical compressive stress increases, the buckling width of ITO seems to be increased. These created cracks are related to well-defined distribution of mechanical stress in ITO island-arrays. We related mechanical bending stress to crack distribution and derived theoretical equation of position-dependent bending stress. And, we verified the bending stress's magnitude to crack distribution observed from optical photographs.

*Keywords* : Compressive, Buckling, crack, Polymer substrate, Bending

## 1. INTRODUCTION

In recent years there has been a growing interest in flexible display devices such as liquid crystal displays (LCD), organic light emitting displays (OLED). Often advantage is gained by making them flexible. The basic way to make flexible displays is to use polymer substrates for carrying the active coatings. However, because indium-tin-oxide (ITO) coating for transparent electrode is brittle component, limited flexibility of the devices exists[1,2]. Our priority is to investigate mechanical stress and failure distribution on ITO coating in flexible deformation (bending)[3-6]. Consequently, it can be realized to maximize flexibility (no fracture) of such a devices composed of brittle materials. In this study, we report the fracture distribution in ITO coating with compressive bending stress on polymer substrates.

## 2. EXPERIMENTAL

We used polycarbonate (PC) film (200  $\mu\text{m}$ ) as substrate of RF-magnetron sputtering system to deposit ITO film (200 nm). The deposition process was carried out at working pressure : 3 mTorr, RF Power : 76 W, deposition time : 20 min. The deposited ITO film's sheet resistance was measured as 35  $\Omega$  /sq. Especially, to investigate position-dependent stress more exactly, the ITO film was patterned for 25 island arrays of 520\*780  $\mu\text{m}^2$  in size. So, this island structure of ITO film was

prepared for the precise analysis of stress dependent conductive failure of the film free of edge force effect resulted from the bulge test. For the convenience, we indicated island arrays as f, e, d, c, b, a from 13rd island (center position) to the edge, respectively[6]. We bent samples of 28 mm\*10 mm size to be the shape of cylindrical by using miniature bending machine[7,8]. And we observed AFM photographs of ITO islands after bending substrates.

## 3. RESULTS AND DISCUSSION

### 3.1 ITO failure mechanism under compressive strain

We applied compressive strain in ITO island-arrays on polymer substrate. Figure 1 shows AFM image at center island of ITO island-arrays with a crack regarding L. The bright region of the center has higher height than that of other region and the buckling width is about 2  $\mu\text{m}$ . From Ref. 1, it is shown that the critical strain under compressive loading is larger than its value under tension. It is expected that compressive loading experiences delamination before cracking. And, after critical strain, resistivity change slope of compressive test is almost same as its value of tensile test. From this fact, it is expected that crack is created from the middle of delaminated buckling region after experiencing delamination. Thereafter, the depth and width of created cracks begin to increase proportionally to applied strain. So, after cracking, ITO delamination region is plastic deformation and no longer elastic deformation. Therefore,

farthest cracked position and crack density are related to imposed mechanical stress in bending. Consequently, the failure mechanism is considered as delamination-buckling-crack. But, because of crack width is very small compared to buckling width (2 $\mu$ m), no resolved crack is observed. From the result of fig. 1, as face-plate distance (L) decreases, the buckling width of ITO seems to be increased. Therefore, the mechanical compressive stress increases, the buckling width of ITO seems to be increased.

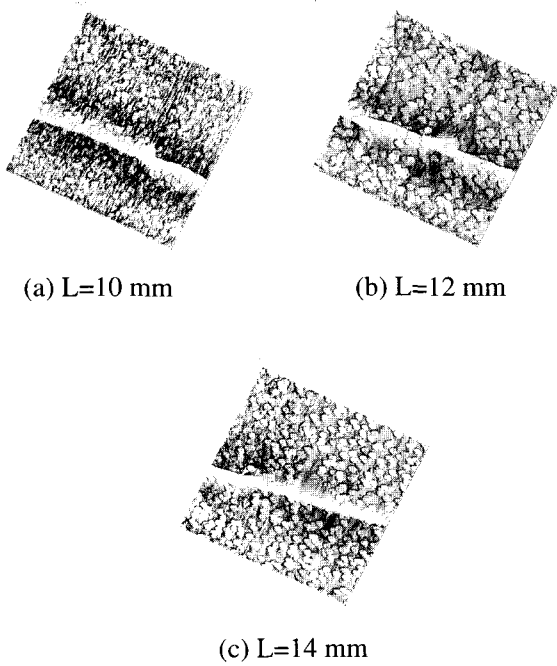


Fig. 1. AFM photograph at center island of ITO island-arrays with crack regarding L.

### 3.2 The theoretical bend geometry

Above discussed bending process can be explained through analysis of the bend geometry that Gulati and Matthewson presented for optical fiber shown in Fig. 2[8].

Curvature radius R at any point along the bend can be given by

$$2\pi R \cdot \frac{d\theta}{2\pi} = ds \quad (1)$$

$$\frac{1}{R} = \frac{d\theta}{ds} \quad (2)$$

where  $\theta$  (radian) is the angle between x axis and tangent at any point and s is running along the fiber axis (in here, neutral line).

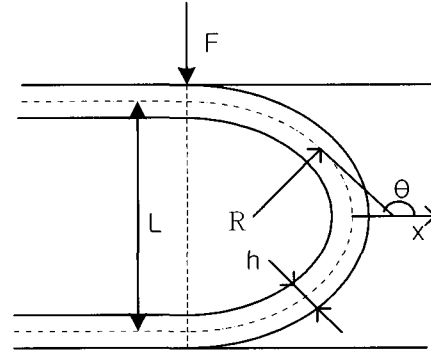


Fig. 2. The geometry of a bend.

From analysis of the moment (bending force) and the bending beam equation and introducing the boundary conditions  $1/R=0$  at the point of force application, the following equations can be derived as

$$\frac{d\theta}{ds} = \sqrt{\frac{2F \sin \theta}{EI}} = \frac{1}{R(\theta)} \quad (3)$$

$$\frac{L}{2} = 0.847 \sqrt{\frac{EI}{F}} \quad (4)$$

$$\ell = 1.854 \sqrt{\frac{EI}{F}} \quad (5)$$

$$F = \frac{b \cdot h^3 \cdot C_b^2 \cdot E}{6L^2} \propto \frac{1}{L^2} \quad (6)$$

$$\sigma(\theta) = r \sqrt{\frac{2EF \sin \theta}{I}} = E \cdot \frac{r}{R(\theta)} \quad (7)$$

in which F is the force [N], E is Young's modulus [Pa],  $C_b$  is geometrical constant (=1.1985), h is sample thickness (200  $\mu$ m), I is the moment of inertia[m<sup>4</sup>],  $\ell$  is half of the length of the total bend, b is sample width (10 mm).

From the fact that  $\theta$  equals to  $\pi/2$  in the center and  $\theta$  equals to  $\pi$  in edge (satisfies condition  $1/R=0$ ) at fixed L (fixed F), it is evident that the stress of the center ( $\theta=\pi/2$ ) is maximum and that of the edge ( $\theta=\pi$ ) is minimum because stress is proportional to  $(\sin \theta)^{1/2}$ . Therefore, the stress is proportionally decreased to  $(\sin \theta)^{1/2}$  as goes to the edge. The important fact is that the farthest bended position ( $1/R=0$ ,  $\theta=\pi$ ) is nearer toward the center position regarding decreased L. Therefore, half of total bend length  $\ell$  decreases proportionally regarding decreased L. This phenomenon can be understood from the bend geometry shown in Fig.

2. Combining eq. (4) and eq. (5), the proportional expression between  $L$  and  $\ell$  can be derived as

$$\ell = \frac{L \cdot 1.854}{2 \cdot 0.847}. \quad (8)$$

Consequently, combining eq. (6) and eq. (7), the following expression can be derived as

$$\sigma(\theta) \propto \frac{\sqrt{\sin \theta}}{L}. \quad (9)$$

### 3.3 The stress distribution corresponding to $\theta$ , $d$ (distance from the center) regarding $L$

Figure 3 (a) shows the stress distribution corresponding to  $\theta$  ( $\pi/2 \leq \theta \leq \pi$ ,  $1.57 \leq \theta \leq 3.14$  (radian)) regarding  $L=10, 12, 14$  mm, respectively. The resultant  $\ell$  is calculated as 10.9445, 13.1334, 15.3223 from eq. (8), respectively. Numerical relationship between  $\theta$  and distance ( $d$ ) far from the center can be considered as

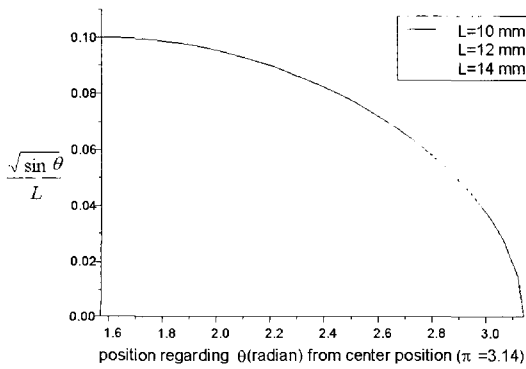
$$d = \left( \frac{\ell}{\pi/2} \theta - \ell \right) = \left( \frac{L \cdot 1.854}{2 \cdot 0.847} \cdot \theta - \frac{L \cdot 1.854}{2 \cdot 0.847} \right) \quad (10)$$

$$= 0.6971 \cdot L \cdot \theta - 1.0944L$$

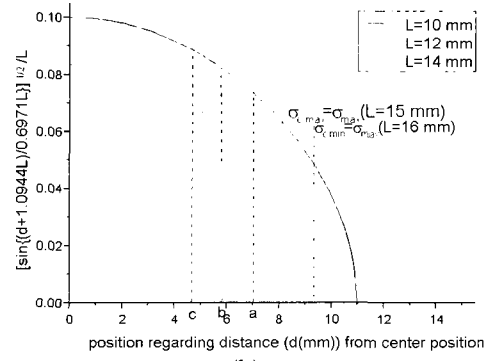
where  $\pi/2 \leq \theta \leq \pi$ ,  $0 \leq d \leq \ell$  and  $d(\theta = \pi/2) = 0$ ,  $d(\theta = \pi) = \ell$  satisfy.

Now, it is available to substitute the stress distribution dependent on  $\theta$  shown in eq. (9) into the stress distribution dependent on  $d$  as follows.

$$\sigma(d) \propto \frac{\sqrt{\sin \theta}}{L} = \frac{\sqrt{\sin \left( \frac{d + 1.0944L}{0.6971L} \right)}}{L} \quad (11)$$



(a)



(b)

Fig. 3. Position-dependent stress distribution regarding two parameters ( $\theta$ ,  $d$ ): (a) stress distribution regarding  $\theta$  (rad); (b) stress distribution regarding distance ( $d$  (mm)) from the center.

Figure 3 (b) shows the stress distribution regarding distance ( $d$  (mm)). A marked a, b, c indicate calculated distance from the center position by using proportional expression. From Fig. 3 (b), at all a, b, c island position, the largest stress is imposed on the ITO islands in case of  $L=10$  mm. As  $L$  decreases, the stress curve of near the edge becomes gradually steeper due to decreased  $\ell$ . As a result, though  $L$  is larger, the more stress than that of small  $L$  is imposed on ITO islands significantly far from the center. But, the critical stress  $\sigma_c$  can not be calculated from above derived equations. Fortunately, it can be considered from empirical results.  $\sigma_{c,max}$ ,  $\sigma_{c,min}$  shown in Fig. 3 (b) is considered through the following crack investigation. On the base of above discussed theory, change of crack density and electrical resistivity was investigated to verify position-dependent stress distribution.

Figure 4 shows crack density at a, b, c, d, e, 13th island position regarding  $L$ . At same island position, the more crack density is observed regarding decreased  $L$ . From this result, it is evident that crack distribution between a and e island position is the same as the stress distribution shown in Fig. 3 (b).

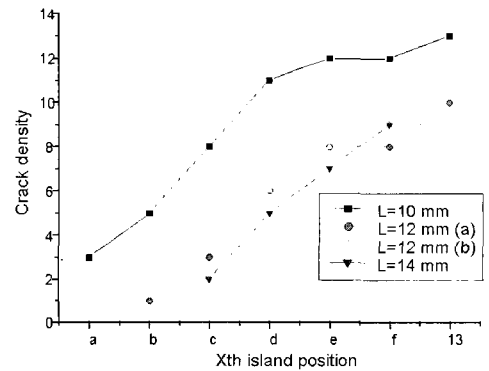


Fig. 4. Crack density at a, b, c, d, e, 13th island position regarding  $L$ .

And from the result of Fig. 4 the critical stress can be derived approximately. So, assuming that the critical stress is imposed on the island of the minimum crack density,  $\sigma_{c:\max}$  can be considered shown in Fig. 3 (b). Because  $\sigma_c$  should be smaller than the stress of c position with  $L=10, 12, 14$  mm. And  $\sigma_{c:\min}$  is considered from the fact that the cracks of  $L=16$  mm are distributed along between 5th and 21st island position. The crack density is one or none along that region. This observance can be considered that near-uniform critical stress is imposed on along between 5th and 21st position. This observance is explained by almost same shape (uniform bending curvature near the center) alike the shape of  $L=18$  mm. From the fact that cracks occur if only the minimum  $\sigma_{\max}$  ( $L = 16$  mm) is imposed on ITO island,  $\sigma_{c:\min}$  can be considered as shown in Fig. 3 (b). Therefore, critical stress is expected to be value between  $\sigma_{\max}$  ( $L = 16$  mm) and  $\sigma_{\max}$  ( $L = 15$  mm).

#### 4. CONCLUSION

Under compressive bending strain, the failure mechanism is delamination-buckling-crack. And, stress distribution of compressive strain is position dependent. The fact that the stress distribution is proportional to  $\sqrt{\sin\theta/L}$  is proved from being the maximum crack density at the center and decreased crack density as goes to the edge. And, As  $L$  decreases, the stress curve of near the edge becomes gradually steeper due to decreased  $\ell$ . As a result, though  $L$  is larger, the more stress than that of small  $L$  is imposed on ITO islands significantly far from the center.

#### ACKNOWLEDGMENTS

This work was supported by National Research Laboratory program (M1-0203-00-0008).

#### REFERENCES

- [1] Z. Chen, B. Cotterell, and W. Wang, "The fracture of brittle thin film on compliant substrates in flexible displays", *Engineering Fracture Mechanics*, Vol. 69, p. 597, 2002.
- [2] Z. Chen, B. Cotterell, W. Wang, E. Guenther, and S. J. Chua, "A mechanical assessment of flexible optoelectronic devices", *Thin Solid Films*, Vol. 394, p. 202, 2001.
- [3] J.-B. Park, J.-Y. Hwang, D.-S. Seo, S.-K. Park, D.-G. Moon, and J.-I. Han, "Position dependent stress distribution of indium-tin-oxide on polymer substrate by external bending force", *Jpn. J. Appl. Phys.*, (submitted).
- [4] S.-K. Park, J.-I. Han, D.-G. Moon, and W.-K. Kim, "Improvement of mechanical property of indium-tin-oxide films on polymer substrates by using organic buffer layer", *Trans. on EEM*, Vol. 3, No. 2, p. 244, 2002.
- [5] J.-B. Park, Y.-G. Lee, J.-Y. Hwang, D.-S. Seo, S.-K. Park, D.-G. Moon, and J.-I. Han, "Study on electrical characteristics of plastic ITO film with bending on multi-barrier films", *J. of KIEEME(in Korean)*, Vol. 17, No. 1, 2004.
- [6] J.-B. Park, J.-Y. Hwang, D.-S. Seo, S.-K. Park, D.-G. Moon, and J.-I. Han, "The stress distribution of indium-tin-oxide (ITO) film on flexible display substrate by bending", *J. of KIEEME(in Korean)*, (submitted).
- [7] P. C. P. Bouten, "Failure test for brittle conductive layers on flexible display substrates", *EURODISPLAY*, p. 313, 2002.
- [8] M. Haenen, "Failure of brittle conductive layers Bending and tensile tests on substrates for flexible displays", *Philips Electronics N. V.* 2002, 2002/801, p. 1.